# Excitation spectrum of a two-dimensional long-range Bose liquid with supersymmetry

E. V. Mozgunov and M. V. Feigel'man
*L. D. Landau Institute for Theoretical Physics, Kosygin Str. 2, Moscow 119334, Russia and*
*Moscow Institute of Physics and Technology, Moscow 141700, Russia*
(Received 3 February 2011; published 21 March 2011)

We have studied the excitation spectrum of the specific two-dimensional model of strongly interacting Bose particles via mapping of the many-body Schrödinger equation in imaginary time to the classical stochastic dynamics. In a broad range of coupling strengths $\alpha$, a roton-like spectrum is found, with the roton gap being extremely small in natural units. A single quantum phase transition between a strongly correlated superfluid and a quantum Berezinsky crystal is found.

DOI: 10.1103/PhysRevB.83.104515 PACS number(s): 05.30.Jp, 05.10.Gg, 74.25.Uv

## I. INTRODUCTION

Usually the system of Bose particles at zero temperature exists in one of two possible ground states: superfluid or crystalline. A more exotic option is the "supersolid" ground state suggested long ago,[1] which attracted a lot of attention recently;[2] this is a state which is expected to possess *both superfluid and crystalline* order simultaneously. Another direction of the search for unusual quantum ground states is related to a search for a "Bose metal," that is, a bosonic analog of a Fermi-liquid; see, for example, Refs. 3 and 4. Such a state would possess *neither superfluid nor crystalline* order. The suggestion to search for such a strange quantum state was made 20 years ago in Ref. 5, in relation to classical thermodynamics of a three-dimensional vortex liquid in high-temperature superconductors. This idea was further developed in Ref. 6 where two different models of a strongly interacting Bose liquid were considered (note that Refs. 5 and 6 refer to continuous two-dimensional (2D) Bose liquids without any lattice, whereas Refs. 3 and 4 consider lattice models). The arguments were given in Ref. 6 in favor of existence of a new, unusual ground state which is still a *liquid* but is *not a superfluid*. One of these models refers to 2D bosons interacting with a 2D dynamic $U(1)$ gauge field, with an effective coupling constant $\sim$1. The second model, of Kane, Kivelson, Lee, and Zhang (KKLZ),[7] is purely static, and it has the remarkable feature that its exact ground-state wave function is represented in a simple Jastrow form.

It was shown later in Ref. 8 that the KKLZ model obeys nonrelativistic supersymmetry, which allows to obtain a number of interesting results analytically. The KKLZ model contains a coupling constant $\alpha$ such that small values $\alpha \leqslant 3$ definitely lead to a gapful superfluid state, whereas at very large $\alpha \geqslant 35$ a kind of a "Berezinsky crystal" with power-law decay of positional correlations is stabilized, according to Ref. 9. An issue was raised in Ref. 8 about the possible existence of a third intermediate ground state of the "normal liquid" type, which could exist in some part of the broad range $3 \leqslant \alpha \leqslant 35$. Supersymmetry of the KKLZ model makes it also possible to compute time-dependent quantum correlation functions via classical Langevin dynamics (the relation between supersymmetry and Langevin dynamics was discussed, in particular, in Ref. 10). A similar approach was proposed by Henley[11] for the lattice quantum systems and used efficiently in Refs. 12 and 13 to explore the excitation spectrum of quantum dimer models on triangular and square lattices at the Rokhsar-Kivelson point.[14] More recently, the same lines of ideas were developed in Ref. 15 for quantum spin models.

In the present paper, we report the results of extensive numerical studies of the dynamic density-density correlation function in the KKLZ model through a broad range of coupling strengths $2 < \alpha < 40$. The presence of a roton-like branch of the excitation spectrum is demonstrated, with the ratio of the roton gap $\Delta$ to the plasma frequency $\omega_0$ strongly decreasing with increase of $\alpha$. Right before the crystallization transition at $\alpha = \alpha_c \approx 37$, this ratio becomes less than $3 \times 10^{-3}$; still we could not identify any finite interval of $\alpha < \alpha_c$ where the roton gap would be exactly zero without a Berezinsky crystal being formed. An effective roton mass $m^*$ defined via the spectrum $\omega(p) = \Delta + (p - p_0)^2/2m^*$ near the roton minimum is found to be weakly dependent upon $\alpha$. The spectral weight $S(p,\omega)$ is well approximated by the single quasiparticle peak at $\omega < 2\Delta$, whereas at higher energies the quasiparticle spectrum is undefined due to the strongly decaying nature of the excitations. Our results support the existence of a superfluid ground state all the way up to the crystallization transition, but the transition temperature $T_c(\alpha)$ scales with $\Delta(\alpha)$ and becomes extremely low at $\alpha$ close to $\alpha_c$.

## II. THE MODEL AND METHOD

We study the KKLZ model of 2D interacting Bose particles characterized by the exact ground-state wave function of Jastrow form

$$\Psi_0(\mathbf{r}_1, \ldots, \mathbf{r}_N) = \text{const} \prod_{j>k} |\mathbf{r}_j - \mathbf{r}_k|^{2\alpha} e^{-\pi\alpha n \sum_i r_i^2}. \quad (1)$$

Here $n$ is the particle density and $\alpha$ is a parameter. Many-body probability density $P_0(\mathbf{r}_1, \ldots, \mathbf{r}_N) = |\Psi_0(\mathbf{r}_1, \ldots, \mathbf{r}_N)|^2$ can be considered as a Gibbs measure for a classical 2D liquid with potential energy

$$V\{\mathbf{r}_i\} = -4\alpha\mathcal{T} \sum_{j>k} \ln|\mathbf{r}_j - \mathbf{r}_k| + 2\pi\alpha\mathcal{T}n \sum_i r_i^2 \quad (2)$$

and temperature $\mathcal{T}$. the quantum Hamiltonian of the KKLZ model is defined as

$$\hat{H} = \sum_j \sum_{\mu=x,y} \hat{q}^\dagger_{j,\mu} \hat{q}_{j,\mu}, \quad \hat{q}_{j,\mu} \equiv i\hbar \frac{\partial}{\partial r_{j,\mu}} + \frac{i}{2} \frac{\partial V}{\partial r_{j,\mu}}, \quad (3)$$

 

where we put $\mathcal{T} = \hbar$ and $2m = 1$. Langevin dynamics leading to the Gibbs distribution $P_0(\mathbf{r}_1, \ldots, \mathbf{r}_N)$ is defined as

$$\frac{dr_{j,\mu}}{dt} = -\frac{\partial V\{\mathbf{r}_i\}}{\partial r_{j,\mu}} + \xi_{j,\mu}(t), \tag{4}$$

where $\overline{\xi_{j,\mu}(t)\xi_{k,\nu}(t')} = 2\mathcal{T}\delta_{jk}\delta_{\mu\nu}\delta(t-t')$. Our goal is to compute the dynamic density-density correlation function $S(\mathbf{k},t) = \frac{1}{\mathcal{V}}\langle n_{\mathbf{k}}(t)n_{-\mathbf{k}}(0)\rangle$ ($\mathcal{V}$ is the system's volume) in the ground state (GS) of the Hamiltonian (3). In terms of spectral expansion it is given by $S(\mathbf{k},t) = \sum_i |\langle \mathrm{GS}|n_{\mathbf{k}}|\mathbf{k},i\rangle|^2 e^{-i\omega_{\mathbf{k},i}t}$, where $i$ denotes all quantum numbers except the momentum $\mathbf{k}$. The equivalence [8,10,11,15] of quantum and classical dynamics for the theories like the one defined by Eq. (3) allows us to use classical simulation of the Langevin dynamics defined in Eq. (4) to compute $S(\mathbf{k},t)$ in the imaginary-time domain: $S(\mathbf{k}, -i\tau) = \mathcal{S}(\mathbf{k},\tau)$, where

$$\mathcal{S}(\mathbf{k},\tau) = \int \prod_j d\mathbf{r}_j(0) d\mathbf{r}_j(\tau) \tag{5}$$

$$\times P(\mathbf{r}_j(0),0,\mathbf{r}_j(\tau),\tau)\frac{1}{\mathcal{V}}\sum_{i,j} e^{ikr_i(\tau)}e^{-ikr_j(0)}, \tag{6}$$

where $P(\mathbf{r}_j(0),0,\mathbf{r}_j(\tau),\tau)$ is the two-time $N$-particle joint distribution function for the stochastic diffusion process defined by Eq. (4). For the derivation of Eq. (6), see Appendix A.

We begin with the application of our computational method to the simpler case of the Calogero-Sutherland model (CSM) [16] defined on a one-dimensional circle of length $L$. The CSM ground-state wave function is $\psi_0 = \prod_{i<j} \sin^{\lambda}(\pi x_{ij}/L)$, where $\lambda > 1/2$, and arbitrary otherwise. The corresponding classical potential energy is $V_{\mathrm{CSM}} = -\lambda \sum_{i<j} \ln \sin^2(\pi x_{ij}/L)$. We simulate the CSM model with $N = 200$ particles via Langevin dynamics to compute its dynamic structure factor $\mathcal{S}(k,\tau)$ and compare with exact results available.[17] According to Ref. 17, CSM spectral density $S(k,\omega) = \sum_i |\langle \mathrm{GS}|A_k|k,i\rangle|^2\delta(\omega_i - \omega)$ is nonzero in a finite region $\omega \in [E_-(k), E_+(k)]$ only, where $E_- = v_s(k - \frac{k^2}{k_0}), E_+ = v_s(k + \frac{k^2}{\lambda k_0})$, and $v_s = \pi\lambda\frac{n}{m}$ and $k_0 = 2\pi n$. In Fig. 1 we plot results of numerical simulation for $\lambda = 2$ together with theoretical low bound curve. In our computation, the lower bound of the spectrum was determined as the extrapolation $E_{\min}(k) = \lim_{t\to\infty} d\ln\mathcal{S}(k,t)/dt$; another spectral characteristic is its simple average $\omega_{\mathrm{fm}}(k) = \int_0^\infty \omega S(\omega,k)d\omega = d\ln\mathcal{S}(k,t)/dt|_{t\to 0}$. The agreement between data for $E_{\min}(k)$ and theoretical spectral boundary $E_-(K)$ is remarkable. It proves the capability of our method to capture gapless excitations with large wave vectors $k \sim k_0$, which are invisible in the "first moment" approximation $\omega_{\mathrm{fm}}$. Note that for small $k \ll k_0$, data for $E_{\min}(k)$ and $\omega_{\mathrm{fm}}(k)$ coincide, as they should for a spectral density nearly saturated by single-particle excitations.

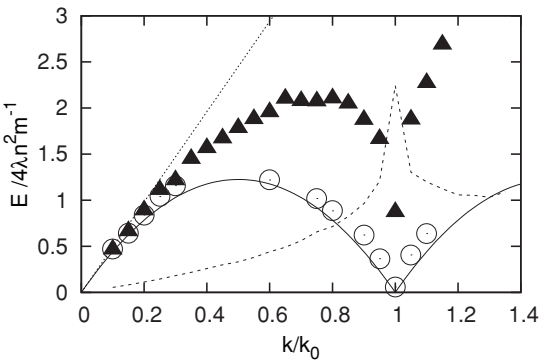


FIG. 1. Computed (CSM) lower bound of the spectrum $E_{\min}(k)$ for $\lambda = 2$ (circles) and results for simple spectral average $\omega_{\mathrm{fm}}(k)$ (triangles). Lines represent the exact theoretical lower bound $E_-(k)$ (solid line), static structure factor $S(k)$ (dashed), and $v_s$ slope (dotted).

## III. THE ROTON GAP AND TRANSITION TO THE QUASI-CRYSTAL

Now we turn to our major subject: the search for low-energy roton modes in the KKLZ model defined by the Hamiltonian (3). An example of the excitation spectrum in the strong coupling region, $\alpha = 20$, is shown in Fig. 2, here and below $N = 256$. We plot here the data for $E_{\min}(k)$ for the wave vectors $k$ in the vicinity of $k_0 = 2\pi\sqrt{n}$, where static structure factor $S(k, t = 0)$ has a peak. The inset to Fig. 2 shows an estimate of $E_{\min}(k)$ in a broad range of $k$ via best fit of $\mathcal{S}(k,\tau)$ to the single exponent $Ae^{-E_1\tau}$. This fitting procedure is slowly converging to the true result, so discrepancies are hard to estimate and therefore not shown. But it still provides a qualitative picture of the excitations in the whole $k$ range. We see that low-$k$ plasma oscillations decay, and their energies can be much lower than exactly known $\omega_{\mathrm{fm}}(k \to 0) = \omega_0$. In the main panel of Fig. 2 we show $E_{\min}(k)$ in the narrow region around $k_0$, obtained via a more accurate fitting procedure, described in Appendix B.

A roton minimum in $E_{\min}(k)$ is clearly visible at $k = k_0$; below we denote the roton gap as $\Delta = E_{\min}(k_0)$. For $\alpha = 20$ the magnitude of the roton gap $\Delta$ is found to be very small, about 1% in comparison with the plasma frequency $\omega_0 = 4\pi\alpha\frac{n}{m}$, which sets a natural energy scale in the problem. In particular, $\omega_0$ is the frequency of the uniform density oscillations in the KKLZ model, see Ref. 8 for details. Thus, our first qualitative observation is that in the strong-coupling region the excitation spectrum shows a very deep roton minimum. As follows from the general arguments,[18] a well-defined excitation spectrum may not exist in the $k$ region where quasiparticle decay is allowed by conservation

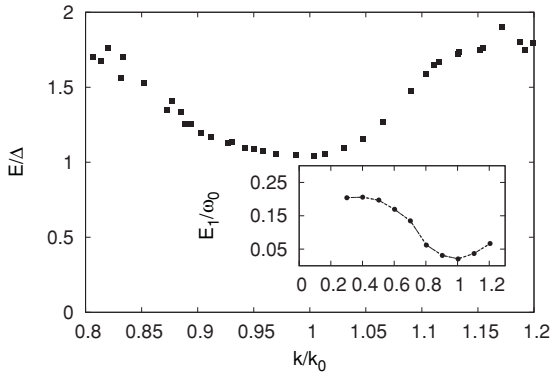


FIG. 2. Quasiparticle energy near the roton minimum for $\alpha = 20$ obtained by the fit of $\mathcal{S}(k,\tau)$; the inset shows a rough estimate (see main text for explanation) for $E(k)$ in the whole $k$ range.

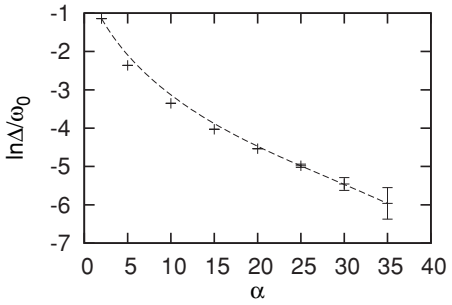


FIG. 3. Roton gap $\Delta$ as function of $\alpha$, logarithmic scale.

laws. For the roton-like spectrum with a deep minimum, the "no-decay" condition is fulfilled at energies $E < 2\Delta$ only: at higher excitation energy, the decay into two rotons is allowed with a high rate. Well-defined roton excitations may exist in the momentum range $p_- < k < p_+$ around the minimal point $k_0$. According to Ref. 18, the excitation energy $E(k)$ is expected to approach the end points $p_\pm$ nonanalytically, with a zero slope:

$$E(k \to p_\pm) = 2\Delta - ae^{-b/|k-p_\pm|}, \tag{7}$$

where $p_\pm$ are called spectrum terminating points, and $a$ and $b$ are some positive constants. Equation (7) results[18] from an exact summation of the most singular diagrams for the momenta $k \approx p_\pm$. Our data presented in Fig. 2 (main panel) are in good qualitative agreement with this prediction. Indeed, we see here two inflection points which are necessary for the $E(k)$ curve to approach the end points with zero slope; these spectrum end points are situated at $(p_-, p_+) \approx (0.8, 1.2)k_0$. Unfortunately, high-precision computation of $E_{\min}(k)$ close to the end points was found to be very difficult due to increasing data scattering.

Similar analysis of the relaxation data for different values of the coupling constant $\alpha$ yields the dependence of the gap magnitude $\Delta$ on $\alpha$, as presented in Fig. 3 in logarithmic scale. Increase of $\alpha$ leads to a very sharp (nearly exponential in the range $10 < \alpha < 35$) decrease of the gap magnitude $\Delta$. The same data for the region of large $\alpha \geqslant 20$ are presented in Fig. 4 in linear scale. These results are consistent with linear vanishing of the gap at $\alpha \approx 37$–$38$, slightly above the point of the crystallization transition $\alpha_{\text{old}} = 35$ found in Ref. 9 for a classical 2D Coulomb gas. However, the values of $\Delta$ in this range contain large relative errors which makes it difficult to determine unambiguously where $\Delta(\alpha)$ vanishes. To approach

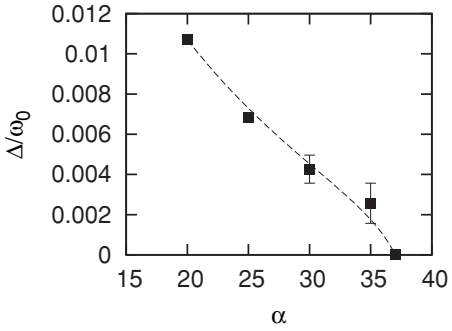


FIG. 4. Ratio of the roton gap to plasma frequency in the large-$\alpha$ range.

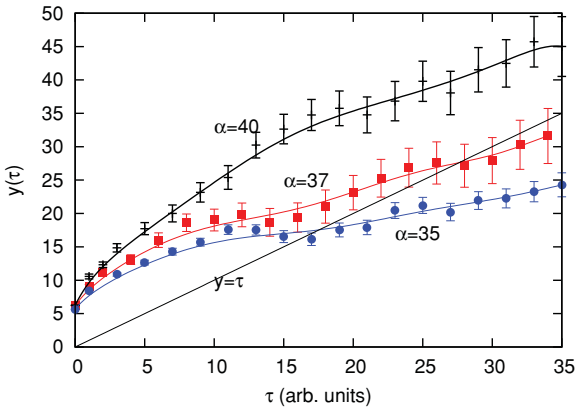


FIG. 5. (Color online) Inverse logarithmic derivative of $\mathcal{S}(k_0,\tau)$ for $\alpha = 35$ (blue dots), 37 (red boxes), and 40 (black bars) as measured directly in the simulation.

the problem of location of the quantum critical point from another perspective, below we compare long-time asymptotics of the dynamic structure factor $\mathcal{S}(k_0,\tau)$ in the liquid and crystalline phases. The crystalline phase of the KKLZ model is very specific. This is a densely packed triangular lattice, but instead of the usual transverse phonons with $\omega \sim q$, it supports phonons with parabolic dispersion, $\omega(q) \sim q^2$. This comes from the fact that the shear modulus of this lattice vanishes itself in the long-wavelength limit, $\mu(q) \propto q^2$, see Ref. 8; here the wave vector $\mathbf{q} = \mathbf{p} - \mathbf{G}_i$, where $\mathbf{G}_i$ is one of principal inverse lattice vectors. The presence of soft shear modes leads to a specific long tail in the time decay of the angle-averaged structure factor $\mathcal{S}(k_0,\tau) = \int \frac{d\varphi}{2\pi}\mathcal{S}(k_0\cos\varphi, k_0\sin\varphi, \tau)$, which can be measured by Langevin dynamics:

$$-\frac{d\ln\mathcal{S}(k_0,\tau)}{d\tau} = \frac{1}{2\tau} - f(\tau), \quad \tau \gg \frac{m^*}{k_0^2}, \tag{8}$$

where $f(\tau) > 0$ decays exponentially with $\tau$ and $m^*$ is the effective mass (to be discussed later). Now we define a function $y(\tau) = -[2d\ln\mathcal{S}(k_0,\tau)/d\tau]^{-1}$ and note that according to Eq. (8) it should never cross the line $y = \tau$. On the other hand, in the liquid phase with a nonzero gap $\Delta$, the function $y(\tau)$ approaches $1/2\Delta$ at $\tau \to \infty$, so its crossing with the straight line $y = \tau$ occurs definitely. In Fig. 5 we present simulation results for the function $y(\tau)$ at $\alpha = 35$, 37, and 40. According to the criterion formulated above, the critical value $\alpha_c$ is also found in the range $37 < \alpha_c < 38$. The data summarized in Figs. 4 and 5 support the conclusion that the liquid state with a small roton gap $\Delta$ transforms into a crystalline state via the single phase transition where $\Delta$ vanishes.

## IV. SUPERFLUID DENSITY AND BKT TRANSITION

Coming back to the discussion of the the gapful liquid phase at $\alpha < \alpha_c$, we note that low-lying excitations with $k \approx k_0$ are characterized, apart from the gap value $\Delta$, by the value of the effective mass $m^* = [d^2E(k)/dk^2|_{k_0}]^{-1}$. Measurement of the $S(k,\tau)$ decay in the vicinity of $k_0$ allows us to determine $m^*$ in a broad range of $\alpha$, as shown in Fig. 6. The results shown in Figs. 4 and 6 yield the parameters of the low-lying excitation spectrum $\varepsilon(k) = \Delta + \frac{(k-k_0)^2}{2m^*}$. Allowing us to determine the temperature of the superfluid-to-normal

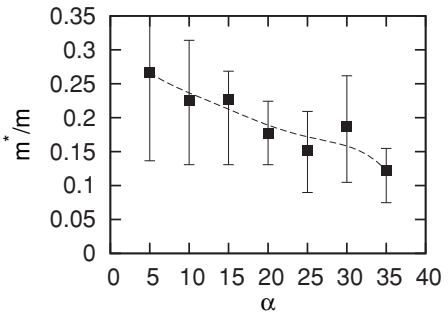


FIG. 6. Quasiparticle mass $m^*$ weakly depends on $\alpha$ even at the transition point.

transition $T_c(\alpha)$. Within the Landau-type mean-field theory $T_c$ is defined as the temperature where superfluid density $n_s = n - n_n$ vanishes. Neglecting quasiparticles interaction, we find the equation for the critical temperature $T_c$:

$$n = -\frac{1}{2m}\int \frac{\partial f_B(\varepsilon,T_c)}{\partial \varepsilon} k^2 \frac{d^2k}{(2\pi)^2}, \tag{9}$$

where $f_B(\varepsilon,T)$ is the Bose distribution function. Evaluation of the integral (9) leads to the result $T_c(\alpha) \approx 0.3\Delta(\alpha)$ valid in the range $10 \leqslant \alpha < \alpha_c$. Note that corrections to $T_c$ due to vortex depairing (the Berezinsky-Kosterlitz-Thouless mechanism) are very weak, due to the smallness of the roton gap $\Delta$ in comparison with the plasma frequency $\omega_0$.

In conclusion, we have computed the excitation spectrum of a 2D Bose liquid with long-range interaction in a strong-coupling regime. A broad range of coupling strengths $\alpha < \alpha_c$ is found where the gapful superfluid state is stable at $T = 0$ in spite of a very small value of the roton gap $\Delta$. Our data suggest a single quantum phase transition from such a strongly correlated superfluid into a quantum crystal phase at $\alpha_c \approx 37$–$38$. At smaller $\alpha$, the superfluid state is stable up to the critical temperature $T_c \approx 0.3\Delta(\alpha)$, which is orders of magnitude lower than a naive estimate $T_0 \sim \hbar^2 n/m$ would give.

## ACKNOWLEDGMENTS

We are grateful to L. B. Ioffe, D. A. Ivanov, L. N. Shchur, and M. A. Skvortsov for useful discussions and advice. This research was supported by the RFBR Grant No. 10-02-00554 and by the RAS Program "Quantum Physics of Condensed Matter."

## APPENDIX A: MAPPING FROM QUANTUM MECHANICS TO CLASSICAL STOCHASTIC EVOLUTION

The standard Fokker-Planck equation corresponding to the Langevin dynamics, Eq. (4), is

$$\dot{P}(\mathbf{r}_1,\ldots,\mathbf{r}_N,t) = \sum_j \frac{\partial}{\partial \mathbf{r}_j}\left(T\frac{\partial}{\partial \mathbf{r}_j} + \frac{\partial V}{\partial \mathbf{r}_j}\right) \times P(\mathbf{r}_1,\ldots,\mathbf{r}_N,t) = \hat{W}P. \tag{A1}$$

The equilibrium solution of Eq. (A1) is given by $P_0 = e^{-V/T}$. One can check that after the change of variables $P = \Psi_0(\mathbf{r}_1,\ldots,\mathbf{r}_N)\Psi(\mathbf{r}_1,\ldots,\mathbf{r}_N,t)$, Eq. (A1) assumes the form of imaginary-time Schrödinger equation $\dot{\Psi} = \hat{H}\Psi$, where Hamiltonian $H$ is constructed from the potential $V$ as shown in Eq. (3). For the following, we denote a position in coordinate space $(\mathbf{r}_1,\ldots,\mathbf{r}_N) \equiv \varphi$ and will not use the specific form of $\hat{H}$. The correspondence of classical and quantum correlation functions that we prove below is valid for any symmetric $H = H^T$ for which the ground state $\Psi_0(\varphi)$ is known exactly. The symmetry condition $H = H^T$ leads to $H^* = H$, which enables us to choose real wave functions, so $P(\varphi,t)$ is always real.

Quantum states form a full system of orthogonal functions:

$$H \to \{\Psi_\lambda(\varphi),\lambda\}, \tag{A2}$$

$$\hat{1} = \sum_\lambda \Psi_\lambda(\varphi)\Psi_\lambda(\varphi') = \delta(\varphi - \varphi'). \tag{A3}$$

Consider the quantum correlation function

$$C_q(t) = \langle\Psi_0|Ae^{-iHt}B|\Psi_0\rangle. \tag{A4}$$

Inserting into the Eq. (A4) the decomposition of the unity operator (A3), we obtain

$$C_q(t) = \sum_\lambda \langle\Psi_0|A|\lambda\rangle e^{-i\lambda t}\langle\lambda|B|\Psi_0\rangle = \int d\varphi d\varphi' \sum_\lambda \Psi_0(\varphi)\Psi_\lambda(\varphi)A(\varphi) \times \Psi_0(\varphi')\Psi_\lambda(\varphi')B(\varphi')e^{-i\lambda t}, \tag{A5}$$

where $A$ and $B$ are diagonal operators (i.e., functions of coordinates $\varphi$ only). The derivation of the quantum-classical mapping begins with replacing variables $P(\varphi,t) = \Psi_0(\varphi')\Psi(\varphi',t)$. The operator governing the classical stochastic evolution is $W = -\Psi_0(\varphi)\hat{H}\frac{1}{\Psi_0(\varphi)}$. It is easy to see that $P_\lambda(\varphi) = \Psi_0(\varphi')\Psi_\lambda(\varphi')$ are the eigenfunctions for this operator, yet this system of eigenfunctions is neither normalized nor orthogonal since the operator $W$ is a non-Hermitian one. Combining the identity $H = H^T$ and the definition of $W$, we obtain $P_0W^T = WP_0$, which is the detailed balance condition.

Rewriting Eq. (A5) formally in classical notation, we find

$$C_q(t) = \int d\varphi d\varphi' \sum_\lambda P_\lambda(\varphi)A(\varphi)P_\lambda(\varphi')B(\varphi')e^{-i\lambda t}. \tag{A6}$$

Now we need to evaluate the classical correlation function. We have the equation for probability density $P(\varphi)$

$$\dot{P} = WP, \tag{A7}$$

and the system is in the equilibrium state $P(t) = P_0$. The two-time correlation function $C(\tau)$ [as given by the right-hand side of Eq. (6)] is defined via stochastic process two-time probability $P(\varphi,0,\varphi',\tau)$ as

$$C(\tau) = \int d\varphi d\varphi' P(\varphi,0,\varphi',\tau)A(\varphi)B(\varphi'), \tag{A8}$$

where $P(\varphi,0,\varphi',\tau) = P(\varphi)p^\tau_{\varphi\to\varphi'}$ according to the definition of a conditional probability $p^\tau_{\varphi\to\varphi'}$ that the system will be in configuration $\varphi'$ at time $\tau$, given that it was in configuration $\varphi$ at time $\tau = 0$. Substituting this expression for $P(\varphi,0,\varphi',\tau)$ into Eq. (A8) we find

$$C(\tau) = \int d\varphi d\varphi' P_0(\varphi)A(\varphi)p^\tau_{\varphi\to\varphi'}B(\varphi'). \tag{A9}$$

To evaluate $p^{\tau}_{\varphi\to\varphi'} = (e^{W\tau})_{\varphi'}\delta(\varphi'-\varphi)$, we need to know the decomposition of the $\delta$ function into eigenmodes. It is convenient to use "quantum" basis (since the classical operator $W$ is non-Hermitian):

$$\delta(\varphi'-\varphi) = \sum_{\lambda} \Psi_{\lambda}(\varphi)\Psi_{\lambda}(\varphi') = \frac{\sum_{\lambda} P_{\lambda}(\varphi)P_{\lambda}(\varphi')}{P_0(\varphi)}. \quad \text{(A10)}$$

Now we can contract this $\delta$ function with $e^{W\tau}$ (remember that eigenvalues are $-\lambda$) to obtain

$$p^{\tau}_{\varphi\to\varphi'} = (e^{W\tau})_{\varphi'}\delta(\varphi'-\varphi) = \frac{\sum_{\lambda} P_{\lambda}(\varphi)P_{\lambda}(\varphi')e^{-\lambda\tau}}{P_0(\varphi)}. \quad \text{(A11)}$$

For the classical correlation function, we obtain

$$C(\tau) = \int d\varphi d\varphi' P_0(\varphi)A(\varphi)\frac{\sum_{\lambda} P_{\lambda}(\varphi)P_{\lambda}(\varphi')e^{-\lambda\tau}}{P_0(\varphi)}B(\varphi')$$
$$= \sum_{\lambda} P_{\lambda}(\varphi)A(\varphi)P_{\lambda}(\varphi')B(\varphi')e^{-\lambda\tau}. \quad \text{(A12)}$$

Comparing Eqs. (A12) and (A6) we find the relation wanted:

$$C_q(t) = C(it). \quad \text{(A13)}$$

## APPENDIX B: DETAILS OF DATA ANALYSIS

For a rotonic spectrum with gap $\Delta$, the quasiparticle continuum begins at $\omega > 2\Delta$. It can be seen by considering two rotons with minimal energy ($k_{1,2} = k_0$) and arbitrary angle between $k_1$ and $k_2$. Total energy is $2\Delta$, and total momentum can be set arbitrarily in the region $K < 2k_0$. Rotons are the only detected excitations below the continuum:

$$S(\omega,k) = A\delta(\omega - E(k)) + S_{\rm con}(\omega,k), \quad \text{(B1)}$$

$$S_{\rm con}(\omega < 2\Delta) = 0, \quad \text{(B2)}$$

$$E(k) \approx \Delta + \frac{(k-k_0)^2}{2m^*} \quad \text{at} \quad k \to k_0. \quad \text{(B3)}$$

In the region $k \in [p_-, p_+]$ we assume the main contribution to come from a quasiparticle, i.e., in Eq. (B1)

$$A \gg \int S_{\rm con}(\omega,k)\, d\omega, \quad \text{(B4)}$$

so that the exact shape of $S_{\rm con}(\omega)$ does not matter. For data fitting we use rectangular spectral density $S_{\rm con}(\omega) = B$, $2\Delta < \omega < \omega_{\max}$, so for each value of $k$ there are four fitting parameters: $A, E(k), B, \omega_{\max}$, apart from the value of $\Delta = E(k_0)$ that is the same for all $k$. We minimize the mean-square deviation $\sum_i [S_{\rm fit}(t_i) - S_{\rm sim}(t_i)]^2$ to find $E(k)$ plotted on Fig. 2. We also check the condition (B4) and find that it is violated in the close vicinity of terminating points, thus the statistical error of determining $E(k)$ grows there.

To collect the data presented in Fig. 3, we do not need to use the $k$ regions near the terminating points $k \approx p_-, p_+$, so we can use inequality (B4) and estimate $E(k)$ just as $d\ln\mathcal{S}/dt|_{t=t_o}$, where $t_o$ is sufficiently long to lead to additional exponential damping of the continuum modes. Note that inaccuracy in determination of $\ln\mathcal{S}$ (and its derivative) grows exponentially with $t_o$, since $1/\mathcal{S} \sim e^{E(k)t_o}$. Therefore the finite simulation time determines how long is the optimal interval $t_o$ we can use. The derivative $d\ln\mathcal{S}/dt$ can be accessed with the use of a Monte Carlo estimator (subtracting the $\mathcal{S}$ values for consequent configurations), or by drawing a line through the sequence of points $\ln\mathcal{S}(t_i), t_i \in [t_o - \delta T/2, t_o + \delta T/2]$. These approaches yield similar results, but the latter is more insightful when one tries to assign error bars $\sigma E(k)$ to the results for $E(k)$. These errors contain a standard $N$-point slope measurement error $\sigma_N E = \sqrt{\frac{12}{N}}\frac{\sigma \ln\mathcal{S}}{\delta T}$ and the systematical overestimating of $E(k)$ due to the continuum modes. The second source of errors is related to the fact that $\ln\mathcal{S}(t_i)$ is not exactly a linear function of time. Assuming that the derivative $d\ln\mathcal{S}/dt$ changes by $\delta E$ in the interval $\delta T$, we can estimate possible systematic errors as $\sigma_c E = \delta E e^{-(2\Delta-E)\delta T/2}/(1 - e^{-(2\Delta-E)\delta T})$. The denominator of this expression diverges while $k$ approach terminating points, which reminds us of the range of applicability of the method we used. Surprisingly, the data analysis using $N$-point treatment of $\ln\mathcal{S}(t)$ and neglecting systematic shift $\sigma_c E$ can be performed in the whole range of $k \in (p_-, p_+)$. This method catches nonanalytic behavior of $E(k)$ near the spectrum terminating points, as well as vanishing of the roton gap $\Delta$ while $\alpha$ approaches $\alpha_c$. In both these cases, error bars $\sigma_N E$ grow considerably, indicating the approach to a transition.


[1] A. F. Andreev and I. M. Lifshits, Sov. Phys. JETP **29**, 1107 (1969).
[2] E. Kim and M. H. W. Chan, Nature (London) **427**, 225 (2004); N. Prokofev and B. Svistunov, Phys. Rev. Lett. **94**, 155302 (2005).
[3] D. Das and S. Doniach, Phys. Rev. B **64**, 134511 (2001).
[4] A. Paramekanti, L. Balents, and M. P. A. Fisher, Phys. Rev. B **66**, 054526 (2002).
[5] M. V. Feigel'man, Physica A **168**, 319 (1990); M. V. Feigel'man, V. B. Geshkenbein, and V. M. Vinokur, Pis'ma Zh. Eksp. Teor. Fiz. **52**, 1141 (1990) [JETP Lett. **52**, 546 (1990)].
[6] M. V. Feigel'man, V. B. Geshkenbein, L. B. Ioffe, and A. I. Larkin, Phys. Rev. B **48**, 16641 (1993).
[7] C. L. Kane, S. Kivelson, D. H. Lee, and S. C. Zhang, Phys. Rev. B **43**, 3255 (1991).
[8] M. V. Feigel'man and M. A. Skvortsov, Nucl. Phys. B **506**, 665 (1997).
[9] Ph. Choquard and J. Clerouin, Phys. Rev. Lett. **50**, 2086 (1983).
[10] M. V. Feigel'man and A. M. Tsvelik, Zh. Eksp. Teor. Fiz. **83**, 1430 (1982) [Sov. Phys. JETP **56**, 823 (1982)].
[11] C. L. Henley, J. Phys. Condens. Matter **16**, S891 (2004).
[12] D. A. Ivanov, Phys. Rev. B **70**, 094430 (2004).
[13] A. M. Läuchli, S. Capponi, and F. F. Assaad, J. Stat. Mech.: Theory Exp. (**2008**) P01010.
[14] D. S. Rokhsar and S. A. Kivelson, Phys. Rev. Lett. **61**, 2376 (1988).
[15] C. Castelnovo, C. Chamon, and D. Sherrington, Phys. Rev. B **81**, 184303 (2010).
[16] F. Calogero, J. Math. Phys. **10**, 2191 (1969); B. Sutherland, *ibid.* **12**, 246 (1971); F. Calogero, Phys. Rev. A **4**, 2019 (1971).
[17] M. Pustilnik, Phys. Rev. Lett. **97**, 036404 (2006).
[18] L. P. Pitaevsky, Zh. Eksp. Teor. Fiz. **36**, 1168 (1959) [Sov. Phys. JETP **39**, 830 (1959)].